Comments on Inorganic Chemistry
Publication details, including instructions for authors and subscription information:
http://www.informaworld.com/smpp/title~content=t713455155

Chiralities of Complexes of BleomycirvType Ligands, a Neglected Feature in Structural Studies Relevant to Anticancer Drug Action

Antonia M. Calafat[a]; Luigi G. Marzilli[a]
[a] Chemistry Department, Emory University, Atlanta, Georgia

To cite this Article Calafat, Antonia M. and Marzilli, Luigi G.(1998) 'Chiralities of Complexes of BleomycirvType Ligands, a Neglected Feature in Structural Studies Relevant to Anticancer Drug Action', Comments on Inorganic Chemistry, 20: 2, 121 — 141
To link to this Article: DOI: 10.1080/02603599808012255
URL: http://dx.doi.org/10.1080/02603599808012255

Chiralities of Complexes of Bleomycin-Type Ligands, a Neglected Feature in Structural Studies Relevant to Anticancer Drug Action

ANTONIA M. CALAFAT and LUIGI G. MARZILLI

Chemistry Department,
Emory University,
Atlanta, Georgia 30322

(Received 01 September, 1997)

Bleomycin (BLM) is a glycopeptide antibiotic used clinically for treating cancers of the head, neck, and testes, as well as certain lymphomas. The anticancer activity of BLM is related to the ability of an iron complex to bind and cleave DNA. High-spin Fe(II)BLM reacts with O_2 to form a short-lived transient species that evolves to "activated BLM," the species responsible for DNA cleavage. In order to gain insight into the possible arrangements of BLM in metal complexes, the coordination properties of BLM have been studied with a variety of metals. Since no X-ray structures of these metallobleomycins (M-BLMs) are known, 2D NMR and/or molecular modeling techniques have provided the most useful insight into the BLM arrangement in M-BLMs. In most proposals, five drug N-donors are arranged around the metal as in a square-pyramid (sp). However, the exact arrangement of the drug and the nature of the ligand donor atoms in M-BLMs is still controversial; the donors usually suggested are the N's from the terminal β-aminoalanine (two amino groups), the pyrimidinylpropionamide (pyrimidine), and the β-hydroxyhistidine (amide and imidazole). In a few cases, metal binding by the mannose carbamoyl group has been proposed. Furthermore, although BLM complexation to any metal creates new chiral centers, few published studies have assessed chirality. Because of some contradictory results and the absence of a comprehensive chirality analysis, we recently chose to examine the coordination of Zn(II) to tallysomycin A (TLMA, a glycopeptide related to BLM). This study led to the proposal of new structural models for ZnTLMA (i.e., sp-basket and

Comments Inorg. Chem.
1998, Vol. 20, No. 2-3, pp. 121-141
Reprints available directly from the publisher
Photocopying permitted by license only

trigonal bipyramid (tbp)) and hence a new ligand arrangement for M-BLMs. These novel ZnTLMA models raise the possibility that the disaccharide (i.e., gulose and mannose) may protect the Fe(II) center in Fe(II)BLM from oxidation until the drug binds to DNA. In this article, the traditional sp and novel sp-basket and tbp arrangements of this type of drug are classified and discussed. Common features are pointed out, along with the significant differences among these arrangements. Since the geometry of the metal-binding domain in M-BLMs may affect the conformation of the rest of the molecule and the binding to DNA, the relevance of the M-BLM structure to the mechanism of drug action is also addressed.

Keywords: *bleomycin, tallysomycin, metal-binding, DNA-binding, structural models, NMR, molecular modeling*

INTRODUCTION

Bleomycins (BLMs, Fig. 1) are a group of glycopeptide antibiotics, with significant anticancer activity.[1] The BLM structure is commonly divided into a metal-binding domain with an attached disaccharide group bearing a carbamoyl moiety, a DNA-binding domain that includes a bithiazole (BIT) moiety and a positively charged tail, and a four-amino-acid residue peptide that links the metal and DNA-binding domains. BLM congeners differ in the nature of the tail.

BLMs cleave oxidatively both DNA[2–5] and RNA[3,6,7] in the presence of redox-active metals and molecular oxygen. High-spin Fe(II)BLM reacts with O_2 to form a short-lived transient species (O_2Fe(II)BLM) that evolves to the species responsible for DNA cleavage, the so-called "activated BLM." Although the exact arrangement of the BLM ligand is not known in this active form responsible for the anticancer activity of BLM, several studies suggest that it is a low-spin, octahedral ferric hydroperoxide complex (HO_2Fe(III)BLM),[8] the only nonheme iron hydroperoxide complex characterized so far.[8–10] This formulation was based on the fact that the electrospray mass spectra (EMS) of the intermediate obtained upon treating Fe(III)BLM with H_2O_2 or Fe(II)BLM with O_2^- was consistent with that of HOO-Fe(III)BLM[9]; the larger mass by 4 Da when Fe(III)BLM reacted with ^{18}O-(H_2O_2) to give HOO-Fe(III)BLM confirmed that this species contained two oxygen atoms derived from hydrogen peroxide and strongly suggested that activated BLM was a ferric peroxide complex.[9] In a separate study, both the pre-edge and edge regions of the Fe K-edge X-ray absorption spectroscopy (XAS) spectra of activated BLM were found to be consistent with a low-spin ferric complex. Furthermore, the pre-edge intensity of acti-

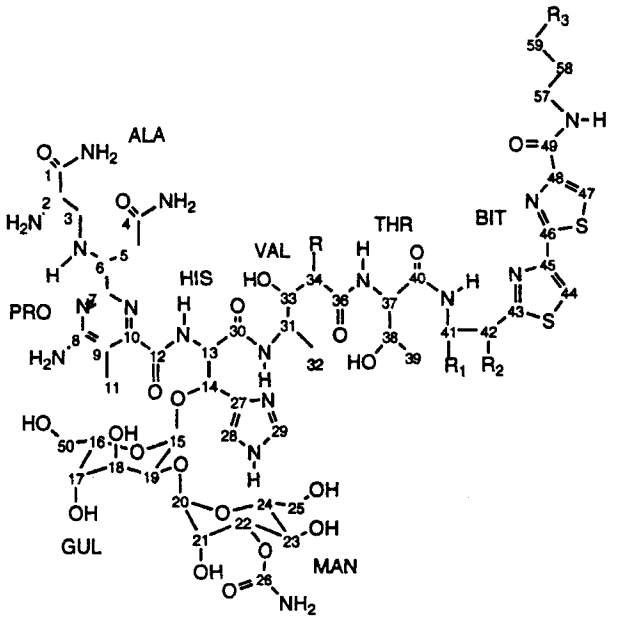

Bleomycin A_2 (BLMA$_2$): R = CH_3

$R_1 = R_2 = H$

$R_3 = (CH_3)_2S^+$

Tallysomycin A (TLMA): R = H

R_1 = TALOSE (TAL)

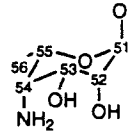

R_2 = OH

$R_3 = CH(NH_2)(CH_2)_2NH(CH_2)_3NH(CH_2)_4NH_2$

FIGURE 1 Bleomycin A_2 and Tallysomycin A

vated BLM did not show the enhancement that would be present if there were a short Fe–O bond (characteristic of an oxo-ferryl species). Therefore, XAS data indicated that activated BLM was a low-spin ferric peroxy complex.[8] Moreover, the wide frequency range and the anisotropy of ^{17}O electron nuclear double resonance (ENDOR) features from activated oxygen in BLM were in marked contrast to the narrow ENDOR feature of an activated oxyferryl oxygen. Finally, the strong hyperfine coupling to one oxygen in the ^{17}O ENDOR spectra was also compatible with end-on ligation of a hydroperoxide,[10] provided that the Fe ligand was a peroxide, as suggested by the EMS[9] and XAS[8] data.

Because no crystal structure of a metal-BLM (M-BLM) complex is known, metal coordination in M-BLMs has been modeled using synthetic BLM analogs. The first model for the metal coordination environment in M-BLMs was derived from the X-ray structure of a Cu(II) complex of P–3A (Fig. 2), a BLM precursor lacking the disaccharide moiety, the peptide linker, and the bithiazole tail.[11] In this structure, the Cu is bound to five N donor atoms in a square pyramidal (sp) environment. The equatorial ligand donors are the β-aminoalanine (ALA) secondary amine (NC3), the pyrimidinylpropionamide (PRO) pyrimidine (NC10), the β-hydroxyhistidine (HIS) amide (NC12), and imidazole (NC29); the ALA primary amine (NC2) occupies the axial site.

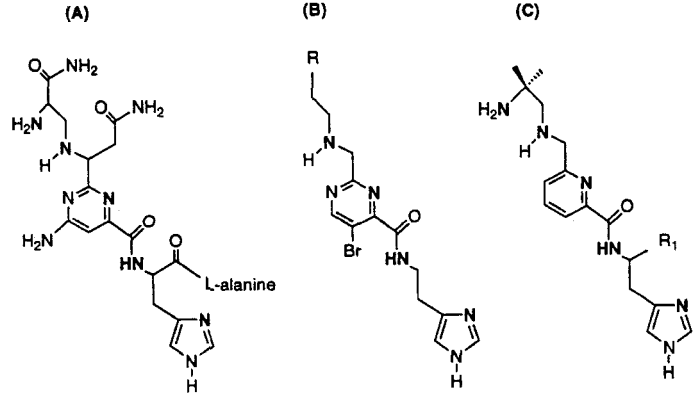

FIGURE 2 BLM ligand analogs. (A) P-3A; (B) R=NH_2 (PMAH), R = $CONH_2$ (PMBH); (C) R_1 = H (ligand analog in Zn tbp X-ray structure), R_1 = t-butyl or lauryl (analogs with bulky substituents)

Subsequent X-ray structures, including those of Cu[12,13] and Co[14–18] bound to a simple BLM analog, PMAH (Fig. 2), have been reported. PMAH contains five nitrogen donor atoms located in the primary and secondary amines, pyrimidine and imidazole rings, and amide; it mimics a major part of the metal-binding domain of BLM, and, like P–3A, lacks some BLM moieties (i. e., disaccharide, peptide linker and bithiazole tail). As for Cu(II)P–3A, the same five N donor atoms in the $[M(PMA)]^+$ models are in an sp arrangement around the metal. In order to model the ALA amide group, the PMBH ligand was synthesized (Fig. 2).[19] Again, the coordination geometry around Cu(II) was a distorted sp. Four nitrogen donors from the pyrimidine, imidazole, secondary amine and deprotonated amide were in the equatorial plane, while the oxygen from the primary amide was the axial ligand. However, the X-band EPR spectrum of $[CuPMB]^+$ was distinctly different from that of Cu(II)-BLM and $[Cu(PMA)]^+$. This result suggested that the ALA amide of BLM does not participate in the coordination to Cu in Cu(II)-BLM at physiological pH.[19]

Other BLM model analogs, similar to PMAH, but with a pyridine ring instead of a pyrimidine, also contain a bulky alkyl group, such as t-butyl or lauryl ($CONH(CH_2)_{11}CH_3$) in place of the BLM disaccharide moiety.[20,21] Although no X-ray structures of these M-BLM analogs have been reported, the electronic spectra were consistent with an sp/5-N-donor metal coordination environment similar to that of Cu(II)P–3A[11] and $[M(PMA)]^+$.[12–18] Both the stability and the oxygen-activating ability of the Fe(II) complexes were enhanced by the introduction of the alkyl group; the Fe(II) complexes showed strong DNA cleaving ability.[20,21]Recently, a new BLM analog with an alkyl group bearing an amide group instead of the disaccharide moiety bearing a carbamoyl group has been synthesized.[22] EPR and electronic spectroscopy data suggest that this ligand coordinates to several divalent metals in an sp-like arrangement. In addition, the shift of the amide ν_{CO} IR band upon Fe(II) complexation was taken to suggest that the amide group may be coordinated to Fe(II).[22]

A Zn(II) BLM-analog complex was recently shown to have a trigonal bipyramidal (tbp) geometry in the solid state with a deprotonated amide as one of the 5 N-donors.[23] Three nitrogen donors from the imidazole, pyridine, and primary amine define the trigonal plane. The apical coordination sites are occupied by the secondary amine and deprotonated amide nitrogens. This ligand used for Zn (Fig. 2) is very similar to pre-

viously used BLM analogs that bind to other metals in an sp arrangement.[24]

In the absence of M-BLM X-ray structures, 2D NMR and molecular modeling studies have provided the most useful insight into the ligand arrangement in M-BLMs. Because the use of NMR for the structural study of activated BLM has several difficulties,[25] other M-BLMs have been analyzed.[26–31] For instance, reports on the solution structures of Co(III)BLMA$_2$ (A$_2$ refers to a derivative with a specific cationic tail)[28,29] and COFe(II)BLMA$_2$,[27] analogs of HO$_2$Fe(III)BLM have appeared. Likewise, NMR studies of the Fe(II)BLM analog, ZnBLMA$_2$,[26] have also been performed. These studies favor as donors the ALA secondary amine, NC3, the PRO pyrimidine nitrogen, NC10, and the HIS deprotonated amide nitrogen, NC12, and an imidazole nitrogen, NC29. There is some controversy regarding the other BLM donors. In particular, some studies consider the ALA primary amine, NC2, as the fifth ligand,[28,29] while others favor the mannose (MAN) carbamoyl group over NC2.[27, 30, 31] Simultaneous binding of NC2 and the MAN carbamoyl nitrogen has also been proposed.[26]

In this article, the various M-BLM structures proposed in the literature are described and analyzed. Common features, as well as the significant differences among them, are pointed out. The recently studied Zn-tallysomycin A (TLMA, a glycopeptide antibiotic closely related to BLM) models are also reviewed. Finally, the relevance of the M-BLM structure in the mechanism of drug action is discussed.

METAL-BLM STRUCTURAL MODELS

Co-BLM Models. In the proposed structures of peroxyCo(III)BLMA$_2$(CoBLMA$_2$ green)[28,29] and aquaCo(III)BLMA$_2$ (CoBLMA$_2$ brown),[28] the BLM coordinates with donors in an sp arrangement with NC3, NC10, the deprotonated amide NC12, and imidazole NC29, as equatorial ligands, and NC2, in the axial site. This arrangement is found in most X-ray structures of M-BLM analogs.[11–18, 24] We shall refer to this type of arrangement as sp I (Fig. 3). CoBLMA$_2$ green[28, 29] is a six-coordinate structure with the hydroperoxide occupying the second axial site in the model. Several long-range NOEs[29] suggested a compact conformation with the BIT and tail folded back underneath the equatorial coordination plane of the Co binding domain

on the same face as the hydroperoxide ligand.[28, 29] Furthermore, the very large ^{1}H and ^{13}C NMR chemical shift changes ($\Delta\delta$) for the methylvalerate (VAL) Me35 and C34H were explained by a well-defined conformation of the VAL and threonine (THR) residues with the VAL directly underneath the imidazole.[28, 29] The MAN residue is located on the top face of the Co equatorial coordination plane, on the same face as the ALA NC2 and relatively far from the HIS moiety (e.g., only an NOE of weak intensity between C22H and C14H is observed).[29] In $CoBLMA_2$ brown,[28] also a six-coordinate structure with water as the sixth ligand, no folding of the BIT was evident. However, the peptide linker folded into definite conformations, as seen in $CoBLMA_2$ green.[28, 29]

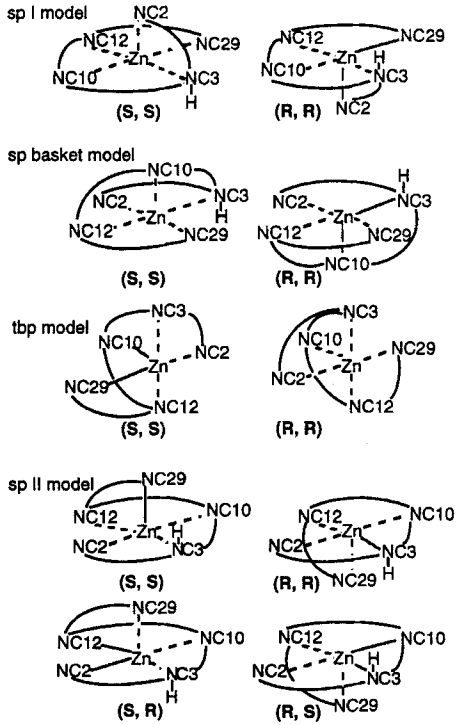

FIGURE 3 All the possible configurations of sp I, sp basket, tbp, and sp II models for the M-BLMs, illustrated with ZnTLMA. Chiralities are indicated in parentheses (Zn, NC3)

Fe-BLM Models. Several models have been proposed for octahedral COFe(II)BLMA$_2$. An early study assessed the BLM ligation sites based on the ^{1}H $\Delta\delta$'s upon formation of COFe(II)BLMA$_2$.[32] The significant ^{1}H $\Delta\delta$'s observed for the ALA and PRO residues, HIS imidazole and MAN C22H were taken to suggest that binding of BLMA$_2$ to Fe involved NC2, NC3, NC10, NC29, and the MAN carbamoyl nitrogen, but not the amide nitrogen NC12.[32] Later, 2D NMR studies, combined with distance geometry calculations, suggested that BLMA$_2$ coordinates to Fe with donors in an sp arrangement with NC3, NC10, NC12 and NC29 as equatorial ligands, and the MAN carbamoyl group in an axial position; the primary amine NC2, in the opposite face of the equatorial coordination plane of the Fe as the disaccharide, was not bound (Fig. 4).[27] However, the authors did not believe the data allowed for a differentiation between coordination through the MAN carbamoyl nitrogen or oxygen atoms. An sp I-like arrangement with a coordinated carbamoyl nitrogen instead of NC2 has also been suggested for ZnBLMA (see below).[30, 31] However, the carbamoyl nitrogen can not be a donor unless it is deprotonated. Therefore, coordination of the carbamoyl nitrogen to the metal is very unlikely. In contrast, resonance Raman studies of FeBLMA$_2$ in the ferric, ferrous, and CO-ligated species indicate that NC10 and NC12 are coordinated in all three species.[33] Recently, the solution structure of the paramagnetic Fe(II)-BLM complex has been investigated by 1D and 2D NMR techniques.[34] The data point toward NC2, NC3, NC10, NC12 and NC29 as ligating atoms to the Fe(II). Although the specific position of the disaccharide in Fe(II)-BLM was not addressed, the reported chemical shifts and T_1 values of the sugar protons for Fe(II)-BLM were taken to conclude that the disaccharide is close, but not bound to the metal.[34] Furthermore, correlation of the Fe(II)-BLM T_1 values[34] with the metal-proton distances derived from the NMR/molecular modeling structure of CoBLMA$_2$ green[29] led the authors[34] to suggest that the structures of these two M-BLMs are similar.

Zn-BLM Models. Although ZnBLMA$_2$ was one of the first metal species to be studied, the different findings compared to other metals and the tbp structure of the Zn-BLM analog[23] have led to a call for further study.[25] Several models differing in coordination geometry have been proposed for ZnBLMA$_2$. Initially, a tetrahedral model was proposed for ZnBLM on the basis of the 1D ^{13}C NMR assignments of BLM and ZnBLM[35] as well as ^{1}H NMR studies of the rates and energy of activa-

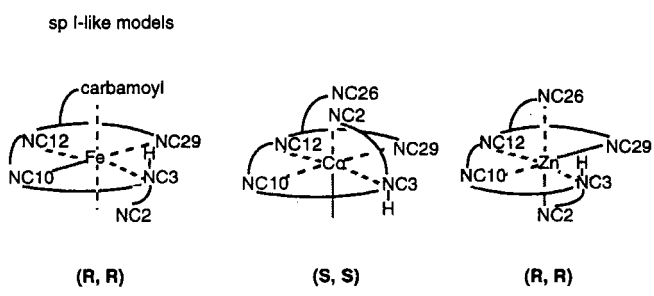

FIGURE 4. Literature proposals having sp I-like $BLMA_2$ arrangements for $COFe(II)BLMA_2$ (left), $CoBLMA_2$ green (center), and $ZnBLMA_2$ (right) showing the position of the carbamoyl group relative to NC2 (unidentate ligands not shown). Chiralities are indicated in parentheses (M, NC3)

tion of dissociation of the ZnBLM complex.[36] Earlier, ^1H $\Delta\delta$'s led to the proposal of an octahedral model for $ZnBLMA_2$[37] with four commonly suggested N donors (NC2, NC3, NC10 and NC29) and two unusual donors: the VAL carbonyl oxygen and the MAN carbamoyl nitrogen. Later, an octahedral model for $ZnBLMA_2$ was constructed by combined 2D NMR and distance geometry methods.[26, 38] BLM binding by five typical N donors in an sp I arrangement (i.e., NC2, NC3, NC10, NC12, and NC29) and the MAN carbamoyl nitrogen as the sixth ligand was advanced in a model based on the ^1H and ^{13}C $\Delta\delta$ observed upon complexation.[26, 38] The coordinated disaccharide and NC2 were on opposite sides of the equatorial coordination plane of the Zn defined by NC3, NC10, NC12, and NC29 (Fig. 4). Later, an sp I-like $BLMA_2$ arrangement analogous to that in $COFe(II)BLMA_2$[27] was assumed in NMR/molecular modeling studies of the adducts of $ZnBLMA_2$[31] and $ZnBLMA_5$[30, 31] with DNA.

Recently, from ^{13}C and ^{113}Cd NMR results on $CdBLMA_2$ at pH 7.6, it was suggested that at most four N donors (from the ALA primary and secondary amines, PRO pyrimidine, and HIS imidazole) were bound to Cd and, by analogy, to Zn in $ZnBLMA_2$.[39] However, earlier work on the complexation of Zn(II) and Cd(II) to macrocyclic oxo polyamine ligands suggested that Zn(II) and Cd(II) behave differently toward coordination with amide nitrogens.[40] For instance, Zn(II) was able to replace an amide hydrogen and form an sp complex at pH < 8. In contrast, the

larger and less acidic Cd(II) displaced the amide proton of the same ligand to give a complex with an sp arrangement only at pH > 10. Therefore, the structure of $CdBLMA_2$ at pH 7.6 may not be the same as that of $ZnBLMA_2$. Furthermore, below we consider the fact that different metals may model either the Fe(II) or the Fe(III) oxidation state. Zn(II) may be useful in assessing Fe(II)BLM's, but it is not clear that Cd(II) is a good model for either Fe oxidation state.

CONTROVERSIAL AND OVERLOOKED FEATURES

Despite continual and extensive research in the M-BLM area, some features remain relatively unexplored and/or are still controversial. Metal complexation to BLM creates the need to assess the two new chiral centers (the metal and the ALA secondary amine, NC3). The donor atoms to the metal and the ligand arrangement as well as the dependence of these features on the metal center are not always clearly defined.

Although chirality in drug-DNA interactions is obviously important, and considerable attention has been paid to the chirality at the asymmetric centers in the antibiotic, only four studies[28, 29, 41, 42] consider the chirality of the metal center (two for M-BLMs,[28, 29] one for ZnTLMA,[41] and one for a M-BLM analog[42]). The only analysis of the chirality of NC3 has been performed on ZnTLMA (see below).[41] In the text, the Cahn-Ingold-Prelog (R and S) system[43, 44] is used to indicate the absolute configuration of the chiral atoms; SS or RR stands for [M(S),NC3(S)] and [M(R),NC3(R)], respectively.[41]

Although it is generally agreed that the ALA secondary amine, NC3, the PRO pyrimidine nitrogen, NC10, and the HIS deprotonated amide nitrogen, NC12, and an imidazole nitrogen, NC29 are donors in M-BLMs, there is some controversy regarding the other BLM donors. As discussed above, some studies suggest the ALA primary amine, NC2, as the fifth ligand,[28, 29] while others favor the MAN carbamoyl group over NC2.[27, 30, 31] Simultaneous binding of NC2 and the MAN carbamoyl nitrogen has also been proposed.[26] However, binding of the MAN carbamoyl group to the metal is strictly dependent on the chirality of the complex. This point was not discussed in the report.

Coordination of the MAN carbamoyl group has been proposed for $ZnBLMA_2$[26, 38] and $COFeBLMA_2$;[27] both models are RR (Fig. 4). The simultaneous coordination of NC2 and the carbamoyl nitrogen, reported

for $ZnBLMA_2$,[26, 38] is possible only in an RR environment. The experimental evidence for the MAN carbamoyl nitrogen coordination in the $ZnBLMA_2$ model included the ^{13}C $\Delta\delta$'s of C15, C19 and C20, a large upfield $\Delta\delta$ for C22H (-0.65 ppm) and the two broad carbamoyl NH singlets (in $BLMA_2$, the carbamoyl NH resonances appeared as one broad signal).[26, 38] Direct coordination of the MAN carbamoyl group to Fe in $COFeBLMA_2$[27] was based on the significant upfield $\Delta\delta$ of C22H (-0.54 ppm) and on the specific orientation of the MAN with respect to the imidazole suggested by the NOE data. This orientation was thought to be favored if the MAN was bound to the Fe.[27] However, the MAN carbamoyl oxygen is a poor donor and thus carbamoyl coordination to the metal, if it exists, should be weak. Moreover, the reported NMR data and T_1 values for Fe(II)BLM[34] are not consistent with coordination of the MAN carbamoyl moiety to Fe(II).[34] In addition, failure to observe ^{113}Cd spin coupling to the MAN C26 in the ^{13}C NMR spectrum of $CdBLMA_2$ makes ligation by the MAN carbamoyl group questionable.[39] Furthermore, recent 2D NMR and molecular mechanics/molecular dynamics (MM/MD) studies of $CoBLMA_2$ green[29] and ZnTLMA[41] have established that the MAN carbamoyl group is not a donor. In both cases, only an SS geometry for the complex can account for the observed NMR constraints.[29, 41] The similarities in ^1H and ^{13}C $\Delta\delta$'s for TLMA and $BLMA_2$ demonstrated that the donor groups to Zn are the same.[41] Therefore, we conducted restrained MM/MD calculations on an octahedral ZnTLMA model similar to that proposed for $ZnBLMA_2$ (NC2, NC3, NC10, NC12 and NC29 in a RR-sp I arrangement and the carbamoyl oxygen was the sixth ligand).[26, 38] As mentioned above, the carbamoyl N cannot bind, but normally an O moiety gives essentially the same structure. Our calculations led to structures in which the chirality at some carbons, including C6, had inverted. Therefore, we believe that the MAN carbamoyl group is not a ligand in any M-BLM.

Zn-TLMA STRUCTURAL MODELS

Because of the issues raised in the preceding section, we investigated the binding of TLMA (tallysomycin A, Fig. 1) to Zn since TLMA was more readily available to us. Tallysomycins (TLMs)[45–47] are closely related to BLMs and bind metals in the same way. TLMs also contain four amino acid residues and a disaccharide moiety. In addition, TLMs

contain an additional sugar, 4-amino-4,6 -dideoxy-L-talose (TAL), and lack a methyl group in one of the amino acid fragments (i.e., VAL). In particular, TLMA, produced by the *Actinomycetes* strain No. E465–94 and first isolated from an Indian soil sample,[45, 46] was shown to induce DNA strand scission.[48] However, BLMs and TLMA have a different site/sequence specificity for DNA cleavage.[49–53] The ^{1}H and ^{13}C NMR spectra of TLMA and $BLMA_2$ and the respective Zn complexes are virtually identical, excluding the tail and the TAL regions;[41] these results confirm that TLMA can be used to model BLM.

In our recent extensive study of ZnTLMA with 2D NMR, NOESY back-calculation methods, and restrained MM/MD calculations,[41] we evaluated several four-coordinate and five-coordinate models. All four-coordinate ZnTLMA models led to strained structures and/or very poor agreement between experimental and calculated NOESY spectra.[41] Four different five-coordinate models were analyzed, namely sp I, sp II, sp basket, and tbp (Fig. 3). In model sp I, TLMA coordinates with NC3, NC10, the deprotonated amide NC12, and imidazole NC29, as equatorial ligands, and NC2, in the axial site; this arrangement is analogous to that of $BLMA_2$ in $CoBLMA_2$ green.[29] In model sp II, NC29 is in an axial position, NC2 occupies an equatorial position, and the other sites are those in the sp I model. This sp II arrangement has been found in a qualitative MM study of Fe(III)-BLM analogs.[42] In the sp basket model, NC10 is in an axial position, and NC2, NC3, NC12 and NC29 occupy the equatorial sites. Finally, in the tbp model, NC3 and NC12 are axial; NC2, NC10 and NC29 form the equatorial plane. This geometry is found in the X-ray structure of a Zn-BLM analog.[23] Because of the chiralities of Zn and NC3, four configurations are hypothetically possible for each model. However, for the sp I, basket and tbp models, only two of the four configurations are feasible since the position of the primary amine dictates the chirality of NC3 (Fig. 3).[41]

After MM/MD calculations, highly distorted imidazole rings and/or very distorted C6 geometries were observed for the SS-sp I and all sp II five-coordinate ZnTLMA models. Although the RR-sp I, RR-basket and RR-tbp models had no distortions and gave good agreement between experimental and back-calculated spectra, the chirality at some carbons, including C6, had inverted. Inversion of the chirality at C6 for the RR-sp I and RR-basket models was caused by an NOE restraint between PRO C6H and MAN C22H (see below). In contrast, for the SS-sp basket and SS-tbp models, neither distorted geometries nor changed chiral-

ities were observed. The unrestrained minimization of the SS-sp I or RR-sp I models indicated that the total potential energy for the SS-sp I model was ~90 kcal/mol lower than for the RR-sp I model. The most significant differences were in the angle, electrostatic, dihedral angle and bond energy terms. The rest of the energy terms (i.e., improper angle, hydrogen bond, van der Waals) and forcing potential (refers to the energy associated with the distance restraints) were similar in both models. From these data, it is clear that the SS model was more stable than the RR model. Restrained MM/MD calculations on the SS-sp I model with no C6H-C22H NOE restraint led to a final restrained structure for which there was good agreement between experimental and calculated NOESY spectra. However, as expected, no C6H-C22H NOE cross-peak was produced in any back-calculated spectra. The absence of this NOE suggests that the carbamoyl group is relatively far away from the Zn-binding domain. Therefore, binding of the carbamoyl group to Zn is unlikely.

The best structural ZnTLMA models, namely SS-sp basket, SS-tbp and SS-sp I, had significant differences in the Zn environment, but comparable Zn–N distances with values in the range found in X-ray structures of five-coordinate Zn(II) complexes.[54] The NOEs between C29H and both C6H and HNC3 in the ZnTLMA models suggested that the HIS imidazole, the ALA and the PRO residues were close to each other. Likewise, these residues were also close to each other in $CoBLMA_2$.[28] Similarly, the ALA secondary amine and the HIS imidazole were directed toward each other in $ZnBLMA_2$[26]and $COFeBLMA_2$.[27] Thus, the coordination of ALA, PRO and HIS imidazole of such antibiotics does not appear to be dependent on the nature of the metal. The absence of long-range NOEs between protons in the metal binding domain and protons in the BIT and tail residues for the ZnTLMA models,[41] $ZnBLMA_2$,[26] $COFeBLMA_2$,[27]and a form of $CoBLMA_2$[28]suggested that the BIT and tail moieties had extended conformations and showed large flexibility in these M-BLMs. In contrast, several long-range NOEs for $CoBLMA_2$ green suggested a compact model with the BIT and tail moieties folded back underneath the equatorial coordination plane of Co.[29] Furthermore, in $CoBLMA_2$ green, the large ^1H and ^{13}C $\Delta\delta$'s for the VAL residue suggested that the VAL and THR residues had a well-defined conformation with the VAL directly underneath the imidazole.[28, 55] The much smaller ^1H and ^{13}C $\Delta\delta$'s for the VAL residue in ZnTLMA,[41] $ZnBLMA_2$,[26] and $COFeBLMA_2$[27] has led to the

suggestion[41, 29] that VAL and THR are in different conformations compared to that for $CoBLMA_2$ green.

Unusual gulose and MAN ^1H and ^{13}C $\Delta\delta$'s have been reported for all M-BLMs[26–29, 38, 39] and for ZnTLMA.[41] In ZnTLMA, the NOE cross-peak between PRO C6H and MAN C22H suggested that the MAN was positioned relatively close to the Zn coordination sphere.[41] This position is probably the result of H-bonding. In the SS-sp basket and SS-tbp ZnTLMA models, hydrogen bonds between HNC3 and OC26, OC4 and HNC26, and OC1 and HOC21 stabilized the position of the disaccharide near the Zn. Likewise, in the SS-sp I model, hydrogen bonding stabilized conformations with Zn and MAN close to each other.[41] However, as mentioned above, the MAN carbamoyl group cannot bind to the metal in an SS model (Fig. 4). Therefore, we believe that the observed disaccharide ^1H and ^{13}C $\Delta\delta$'s in M-BLMs reflect the change in conformation and positioning of the disaccharide upon complexation[41] and not coordination of the carbamoyl group.

These SS-sp I, SS-sp basket and SS-tbp ZnTLMA models were all able to explain most of the experimental data. However, several factors led us to consider the SS-sp I arrangement to be unlikely for Zn, especially the arrangement's failure to account for the C6H-C22H NOE.[41] For ZnTLMA, this NOE is present even at 100 ms; interestingly, although the authors made no mention of this cross-peak, it can also be observed in the published NOESY spectrum of $ZnBLMA_2$.[26] In contrast, it is not present in the published spectrum of $COFeBLMA_2$.[27] Relevant spectral data were not published for $CoBLMA_2$.[28, 29]

The SS-sp basket and SS-tbp ZnTLMA models gave this key NOE. The potential energy for the SS-sp basket model was lower than for the SS-tbp model, and we concluded that the SS-sp basket model best represents the structure of ZnTLMA.[41] Because the NMR data demonstrate that ZnTLMA[41] and $ZnBLMA_2$[26] must have the same overall structure, we proposed that $ZnBLMA_2$ also has this novel SS-sp basket geometry. However, we could not rule out a structure intermediate between the basket and tbp structures for ZnTLMA and $ZnBLMA_2$.

IMPLICATIONS AND ISSUES RAISED BY THE NEW MODEL

The sp-basket and tbp ZnTLMA structures raise a number of interesting questions. First, why have both of these related structural models been

overlooked in the past? Second, why are there no simple models with similar structures? Third, what are the implications concerning the Fe(II) derivatives of the BLM family of drugs and the conversion of the Fe(II) to the activated Fe(III) form? Fourth, what is the relevance of the novel drug arrangements to those previously proposed for DNA-bound Fe-BLMs? We have offered answers to the first two questions in an earlier report,[41] and we summarize only salient features here. A discussion of the third and fourth issues follows below.

To address the first two questions, we stress that previous studies have focused on metals that favor specific geometries stabilized by crystal field effects. Normally the chelate rings on either side of a coordinated deprotonated amide would lie in the same coordination plane. Thus, in previous modeling studies these arrangements were not evaluated. However, the large chelate ring involving imidazole permits the two novel arrangements, and there is no ligand field stabilization for Zn(II). The tbp Zn synthetic model differs from ours, we believe, because the metal binding domain has no attached bulky groups like those present in the antibiotic itself (disaccharide and peptide linker).

ACTIVATION AND BINDING

The ultimate goal in studying structures of M-BLMs is to understand how the structure influences the mechanism by which M-BLMs cleave DNA, particularly both strands of DNA.[25] This cleavage is preceded by at least two initial processes, the activation of the Fe center and the DNA binding. These could be either separate events or concerted processes. The interactions between several M-BLMs and oligonucleotides have been studied as models for DNA binding by Fe-BLMs.[3, 30, 31, 55–62] Here we consider only these prior steps and not the subsequent reactions.

There is good reason to believe that TLMA or BLMs can adopt the novel SS-sp basket arrangement when bound to Fe(II). If O_2 approaches the SS-sp basket (or SS-tbp) Fe(II)BLM from the NC10FeNC29 edge, activated six-coordinate HO_2Fe(III)BLM with an SS-sp I BLM arrangement (analogous to the $CoBLMA_2$ green model[28, 29]) would form. If O_2 approaches different edges, the resulting ligand arrangement would be SS-sp II or SS-sp basket. An RR arrangement as proposed for $ZnBLMA_2$[26] and $COFeBLMA_2$[27] cannot be formed, other than in the unlikely inversion of the chirality both at metal and at NC3.

In the SS-sp basket and SS-tbp models,[41] the hydrogen-bond network positions the disaccharide so that it covers the potential sixth coordination site. MM/MD calculations on a six-coordinate ZnTLMA structure with an SS-sp basket arrangement and with H_2O or O_2 as the sixth axial ligand suggested that an SS-sp basket six-coordinate model is feasible.[41] Nevertheless, the position of the disaccharide in the SS-sp basket arrangement would impede the loss or approach of a sixth ligand, e.g., O_2. The lower affinity for CO binding and a much slower rate of CO rebinding reported[63] for $FeBLMA_2$ compared to an FeBLM analog lacking the sugars bear on this point. H-bonding of the carbamoyl group to PRO amide groups was invoked to explain the stabilization of a $FeBLMA_2$ conformation in which the disaccharide provided a steric environment similar to those of iron "capped" porphyrins.[63] The chiralities of the metal and NC3 were not discussed, but the structure proposed to cap the site clearly has RR stereochemistry. The SS-sp basket we proposed earlier[41] has the relevant chirality and also explains the CO binding data.

Compared to analogs with a hydrogen in place of the disaccharide moiety, analogs with a bulky alkyl group at this point have enhanced stability for the Fe(III) complexes (e.g., no precipitation of $Fe(OH)_3$) perhaps because the alkyl group creates a hydrophobic cavity around the metal and/or covers the sixth coordination site.[20, 21] These Fe(III)-BLM analogs had a smaller DNA cleaving activity than Fe-BLM. This behavior was explained reasonably well by the absence in these BLM analogs[20, 21] of an apparent DNA binding site, such as the BIT moiety. However, these Fe-BLM analog complexes exhibited considerable oxygen activating ability, perhaps because they lack H-bonding groups in the substituent. Similarly, disruption of the hydrogen-bond network on DNA bonding could facilitate the reaction between O_2 and an SS-sp basket Fe(II)BLM species and lead to the formation of activated BLM with an SS-sp basket arrangement. However, if the BLM activated form has the SS-sp I arrangement, the O_2 would have to approach the SS-sp basket Fe(II)BLM from the direction of the NC10FeNC29 edge, and this would require a rearrangement; this rearrangement could be facilitated by DNA binding.

There are two important series of studies of M-BLM derivatives bound to DNA oligonucleotides.[30, 31, 55, 58] In one, utilizing $ZnBLMA_2$ (and the close analog $ZnBLMA_5$),[30, 31] the emphasis was placed on the changes in the DNA conformation and on the interaction of the BIT

moiety with the DNA. The dynamic nature of the adducts led to few intermolecular NOEs useful in defining the metal-binding domain and its interaction with DNA. In a second series, the $CoBLMA_2$ green form interaction with DNA was assessed.[55, 58, 62] NOESY data on the interaction of $CoBLMA_2$green with $d(CCAGGCCTGG)_2$ suggest that the Co complex binds in slow exchange with DNA and the BIT moiety is partially intercalated between base pairs $C_6G_{15}$and C_7G_{14} adjacent to the GpC cleavage site.[55, 58] Likewise, 2D NMR data on the interaction of $CoBLMA_2$ green with $d(GGAAGCTTCC)_2$ and $d(AAACGTTT)_2$ are consistent with intercalation of the BIT moiety into the base pair structure of the $CoBLMA_2$-DNA adduct.[62] In these two separate $CoBLMA_2$ studies,[55, 58, 62] upon binding to DNA, the metal-binding domain is in close proximity to G5, the coordinated peroxide occupies a position between G5 and C6 or T6, and the BIT intercalates between the base pairs at positions 6 and 7.[55, 58, 62]

The large number of NOEs in the $CoBLMA_2$-DNA studies[55, 58] allows us to make a useful comparison with the ZnTLMA results.[41] The $CoBLMA_2$-DNA adduct had many intermolecular NOEs that defined the parts of the metal-binding domain closest to the DNA and also the orientation of the complex with respect to the DNA. Specifically, the ALA and PRO parts of the metal-binding domain interacted most intimately with the DNA, in the minor groove. These parts of the three SS models (i.e., sp I, basket and tbp) are very similar, with differences in the less well-defined termini of the amide chains, which in general were not restrained. Many other contacts between the drug model and the DNA involved the flexible and less well-defined parts of the ZnTLMA models. Judging from the information available, we believe it is possible that the metal domain of an SS-sp basket active Fe-BLM could interact with the DNA in a similar way as in the SS-sp I $CoBLMA_2$-adduct, provided the disaccharide was displaced from covering the sixth coordination site. The disaccharide in the bound $CoBLMA_2$ green form and that in the SS-sp I ZnTLMA model occupy very similar positions. Not only does the disaccharide have to move to allow the ready approach of O_2, it must also move to permit the proposed DNA-binding of $CoBLMA_2$ green form. Recent data support this hypothesis.[34]Analysis of the proton-metal distances derived from the $CoBLMA_2$ green structure bound to DNA[55] has led to the suggestion that the MAN moiety alters its conformation significantly upon DNA binding,[34] perhaps as a result of the considerably larger flexibility for the MAN residue when

compared to the rest of BLM moieties.[34] Thus, it is interesting to hypothesize that such movement of the disaccharide moiety could facilitate formation of the BLM activated form when Fe(II)BLM binds to DNA. This would be an efficient mechanism since activation and cleavage would be closely coupled.

CONCLUSIONS

In summary, several arrangements of TLMA (and by analogy, BLM) have been critically assessed. If Fe(II)BLM had the novel SS-sp basket or SS-tbp arrangement described recently for ZnTLMA, addition of O_2 could yield products with BLM in an SS-sp I arrangement suggested for activated BLM (HO_2Fe(III)BLM) in work on $CoBLMA_2$ green. In these novel arrangements, the disaccharide covers the sixth coordination site and cannot bind to the metal. Furthermore, the disaccharide must move to allow rearrangement to the DNA binding mode proposed for activated Fe-BLM in studies of $CoBLMA_2$ green. This rearrangement raises intriguing possibilities that activation, binding, and cleavage could be linked, especially *in vivo*. However, we know of no firm data to support this hypothesis. Nevertheless, we believe this hypothesis should be considered among alternative possibilities, particularly in studies aimed at testing the mechanism of double-strand cleavage, since the bound Fe-BLM needs to be reactivated for the second cleavage event.

This hypothesis that new arrangements exist was driven by the need to explain as much of the spectroscopic data as possible concerning the ZnTLMA and $ZnBLMA_2$ complexes. These complexes have properties that are very similar to those of other metals. A complete understanding of the structure to the level needed to interpret function requires that all spectroscopic features be explained. However, observations such as the large shifts of C22H and C5 on binding to several metals are not clearly explained by any current models. These shifts could arise from an odd conformation adopted by the free drug, but this possibility needs to be verified. There are, nevertheless, clear differences between adducts of different metals. Potential differences in binding mode of Zn and Cd and different NOE patterns between Co and Zn and even between different Co forms have been mentioned above. Additional studies are needed to assess these differences. For example, complexes with Co(III), Zn(II), Cd(II), and Fe(II)CO containing more elaborate ligand analogs for BLM

having bulky substituents could be investigated. Also, spectroscopic solution studies are needed to evaluate such complexes for comparison to available information on complexes of the antibiotics.

Acknowledgments

This work was supported by NIH grant GM 29222 to L.G.M. L.G.M. thanks the Japan Society for the Promotion of Science for a Fellowship which facilitated the preparation of the manuscript. We thank Drs. M. Shionoya (Institute for Molecular Science, Okazaki), E. Kimura and T. Koike (Hiroshima), M. Goto and H. Kurosaki (Kumamoto), and Y. Sugiura (Kyoto) for useful discussions.

References

1. H. Umezawa, K. Maeda, T. Takeuchi and Y. Oakami, J. Antibiot. A **19**, 200–209 (1966).
2. D. H. Petering, Q. K. Mao, W. B. Li, E. Derose and W. E. Antholine, in *Metal Ions in Biological Systems*, Vol. 33, A. Sigel and H. Sigel, Eds. (Marcel Dekker, New York, NY, 1996), pp. 619–648.
3. S. A. Kane and S. M. Hecht, in *Progress in Nucleic Acid Research and Molecular Biology*, Vol. 49, W. E. Cohn and K. Moldave, Eds. (Academic Press Inc., San Diego, CA, 1994), pp. 313–352.
4. D. H. Petering, R. W. Dyrnes and W. E. Antholine, Chem.-Biol. Interactions **73**, 133–182 (1990).
5. J. Stubbe and J. W. Kozarich, Chem. Rev. **87**, 1107–1136 (1987).
6. J. M. Battigello, M. Cui and B. J. Carter, in *Metal Ions in Biological Systems*, Vol. 33, A. Sigel and H. Sigel, Eds. (Marcel Dekker, New York, NY, 1996), pp. 593–617.
7. C. E. Holmes and S. M. Hecht, J. Biol. Chem. **268**, 25909–25913 (1993).
8. T. E. Westre, K. E. Loeb, J. M. Zaleski, B. Hedman, K. O. Hodgson and E. I. Solomon, J. Am. Chem. Soc. **117**, 1309–1313 (1995).
9. J. W. Sam, X. J. Tang and J. Peisach, J. Am. Chem. Soc. **116**, 5250–5256 (1994).
10. A. Veselov, H. J. Sun, A. Sienkiewicz, H. Taylor, R. M. Burger and C. P. Scholes, J. Am. Chem. Soc. **117**, 7508–7512 (1995).
11. Y. Iitaka, H. Nakamura, T. Nakatani, Y. Muraoka, A. Fujii, T. Takita and H. Umezawa, J. Antibiot. **31**, 1070–1072 (1978).
12. S. J. Brown, S. E. Hudson, D. W. Stephan and P. K. Mascharak, Inorg. Chem. **28**, 468–477 (1989).
13. S. J. Brown, P. K. Mascharak and D. W. Stephan, J. Am. Chem. Soc. **110**, 1996–1997 (1988).
14. E. Farinas, J. D. Tan, N. Baidya and P. K. Mascharak, J. Am. Chem. Soc. **115**, 2996–2997 (1993).
15. J. D. Tan, S. E. Hudson, S. J. Brown, M. M. Olmstead and P. K. Mascharak, J. Am. Chem. Soc. **114**, 3841–3853 (1992).
16. S. J. Brown, M. M. Olmstead and P. K. Mascharak, Inorg. Chem. **28**, 3720–3728 (1989).
17. M. Muetterties, P. K. Mascharak, M. B. Cox and S. K. Arora, Inorg. Chim. Acta **160**, 123–134 (1989).

18. S. J. Brown, S. E. Hudson and P. K. Mascharak, J. Am. Chem. Soc. **111**, 6446–6448 (1989).
19. L. A. Scheich, P. Gosling, S. J. Brown, M. M. Olmstead and P. K. Mascharak, Inorg. Chem. **30**, 1677–1680 (1991).
20. K. Shinozuka, H. Morishita, T. Yamazaki, Y. Sugiura and H. Sawai, Tetrahedron Lett. **32**, 6869–6872 (1991).
21. J. Kohda, K. Shinozuka and H. Sawai, Tetrahedron Lett. **36**, 5575–5578 (1995).
22. T. Arai, K. Shinozuka and H. Sawai, Bioorg. Medicinal Chem. Lett. **7**, 15–18 (1997).
23. H. Kurosaki, K. Hayashi, Y. Ishikawa and M. Goto, Chem. Lett. 691–692 (1995).
24. E. Kimura, H. Kurosaki, Y. Kurogi, M. Shionoya and M. Shiro, Inorg. Chem. **31**, 4314–4321 (1992).
25. J. Stubbe, J. W. Kozarich, W. Wu and D. E. Vanderwall, Account Chem. Res. **29**, 322–330 (1996).
26. M. A. J. Akkerman, C. A. G. Haasnoot and C. W. Hilbers, Eur. J. Biochem. **173**, 211–225 (1988).
27. M. A. J. Akkerman, E. W. J. F. Neijman, S. S. Wijmenga, C. W. Hilbers and W. Bermel, J. Am. Chem. Soc. **112**, 7462–7474 (1990).
28. R. X. Xu, D. Nettesheim, J. D. Otvos and D. H. Petering, Biochemistry **33**, 907–916 (1994).
29. W. Wu, D. E. Vanderwall, S. M. Lui, X. J. Tang, C. J. Turner, J. W. Kozarich and J. Stubbe, J. Am. Chem. Soc. **118**, 1268–1280 (1996).
30. R. A. Manderville, J. F. Ellena and S. M. Hecht, J. Am. Chem. Soc. **116**, 10851–10852 (1994).
31. R. A. Manderville, J. F. Ellena and S. M. Hecht, J. Am. Chem. Soc. **117**, 7891–7903 (1995).
32. N. J. Oppenheimer, L. O. Rodriguez and S. M. Hecht, Proc. Natl. Acad. Sci. USA **76**, 5616–5620 (1979).
33. S. Takahashi, J. W. Sam, J. Peisach and D. L. Rousseau, J. Am. Chem. Soc. **116**, 4408–4413 (1994).
34. T. E. Lehmann, L. J. Ming, M. E. Rosen and L. Que, Biochemistry **36**, 2807–2816 (1997).
35. J. C. Dabrowiak, F. T. Greenaway and R. Grulich, Biochemistry **17**, 4090–4096 (1978).
36. R. E. Lenkinski and J. L. Dallas, J. Am. Chem. Soc. **101**, 5902–5906 (1979).
37. N. J. Oppenheimer, L. O. Rodriguez and S. M. Hecht, Biochemistry **18**, 3439–3445 (1979).
38. M. A. J. Akkerman, C. A. G. Haasnoot, U. K. Pandit and C. W. Hilbers, Magn. Reson. Chem. **26**, 793–802 (1988).
39. J. D. Otvos, W. E. Antholine, S. Wehrli and D. H. Petering, Biochemistry **35**, 1458–1465 (1996).
40. E. Kimura, T. Koike, T. Shiota and Y. Iitaka, Inorg. Chem. **29**, 4621–4629 (1990).
41. A. M. Calafat, H. Won and L. G. Marzilli, J. Am. Chem. Soc. **119**, 3656–3664 (1997).
42. Y.-D. Wu, K. N. Houk, J. S. Valentine and W. Nam, Inorg. Chem. **31**, 718–720 (1992).
43. R. S. Cahn, C. Ingold and V. Prelog, Angew. Chem. Int. Ed. Engl. **5**, 385–415 (1966).
44. R. J. Fessenden and J. S. Fessenden, *Organic Chemistry* (Brooks/Cole, Belmont, CA, 1986).
45. H. Kawaguchi, H. Tsukiura, K. Tomita, M. Konishi, K. Saito, S. Kobaru, K. Numata, K. Fujisawa, T. Miyaki, M. Hatori and H. Koshiyama, J. Antibiot. **30**, 779–788 (1977).

46. M. Konishi, K. Saito, K. Numata, T. Tsuno, K. Asama, H. Tsukiura, T. Naito and H. Kawaguchi, J. Antibiot. **30**, 789–805 (1977).
47. T. Miyaki, O. Tenmyo, K.-I. Numata, K. Matsumoto, H. Yamamoto, Y. Nishiyama, M. Ohbayashi, H. Imanishi, M. Konishi and H. Kawaguchi, J. Antibiot. **34**, 658–664 (1981).
48. J. E. Strong and S. T. Crooke, Cancer Res. **38**, 3322–3326 (1978).
49. C. Mirabelli, S. Mong, C.-H. Huang and S. T. Crooke, Biochem. Biophys. Res. Commun. **91**, 871–877 (1979).
50. C. K. Mirabelli, C.-H. Huang, A. W. Prestayko and S. T. Crooke, Cancer Chemother. Pharmacol. **8**, 57–65 (1982).
51. C. K. Mirabelli, W. G. Beattie, C.-H. Huang, A. W. Prestayko and S. T. Crooke, Cancer Res. **42**, 1399–1404 (1982).
52. C. K. Mirabelli, A. Ting, C.-H. Huang, S. Mong and S. T. Crooke, Cancer Res. **42**, 2779–2785 (1982).
53. C. K. Mirabelli, C.-H. Huang and S. T. Crooke, Biochemistry **22**, 300–306 (1983).
54. A. Vedani and D. W. Huhta, J. Am. Chem. Soc. **112**, 4759–4767 (1990).
55. W. Wu, D. E. Vanderwall, C. J. Turner, J. W. Kozarich and J. Stubbe, J. Am. Chem. Soc. **118**, 1281–1294 (1996).
56. R. J. Duff, E. Devroom, A. Geluk, S. M. Hecht, G. A. Vandermarel and J. H. Vanboom, J. Am. Chem. Soc. **115**, 3350–3351 (1993).
57. V. F. Zarytova, D. S. Sergeyev and T. S. Godovikova, Bioconj. Chem. **4**, 189–193 (1993).
58. W. Wu, D. E. Vanderwall, J. A. Stubbe, J. W. Kozarich and C. J. Turner, J. Am. Chem. Soc. **116**, 10843–10844 (1994).
59. M. J. Absalon, J. W. Kozarich and J. Stubbe, Biochemistry **34**, 2065–2075 (1995).
60. M. J. Absalon, W. Wu, J. W. Kozarich and J. Stubbe, Biochemistry **34**, 2076–2086 (1995).
61. S. A. Kane, S. M. Hecht, J. S. Sun, T. Garestier and C. Helene, Biochemistry **34**, 16715–16724 (1995).
62. Q. K. Mao, P. Fulmer, W. B. Li, E. F. Derose and D. H. Petering, J. Biol. Chem. **271**, 6185–6191 (1996).
63. Y. Sugiura, J. Kuwahara and T. Suzuki, FEBS Lett. **182**, 39–42 (1985).